Research Square

Preprints are preliminary reports that have not undergone peer review.
They should not be considered conclusive, used to inform clinical practice,
or referenced by the media as validated information.

Lead Exposure Induced Copper Clearance Disorder of Blood-CSF Barrier

Bin He
North China University of Science and Technology
Liyuan Wang
North China University of Science and Technology
Shuang Li
North China University of Science and Technology
Fuyuan Cao
North China University of Science and Technology
Lei Wu
North China University of Science and Technology
Song Chen
North China University of Science and Technology
Shulan Pang
North China University of Science and Technology
Yanshu Zhang (yanshuzhang@ncst.edu.cn)

Research

Keywords: lead, copper, blood-CSF barrier, copper transport, CSF

Posted Date: July 23rd, 2020

DOI: https://doi.org/10.21203/rs.3.rs-41556/v1

License: This work is licensed under a Creative Commons Attribution 4.0 International License.
Read Full License

Abstract

Lead is a heavy metal commonly found in the environment with known neurotoxicity, hematological and other toxicities. It has been found that lead exposure can disturb partial metal regulatory function in the blood-CSF barrier (BCB). Copper, which play an important role in maintaining normal brain function, can accumulate in brain after lead exposure. The studies of Alzheimer's disease (AD) indicated that abnormal copper homeostasis in cerebrospinal fluid (CSF) may be involved in the pathogenesis. However, the mechanism of copper disturbance in the brain caused by lead is still unknown. This study was designed to investigate copper clearance by the BCB in central nervous system after lead exposure, with focus on copper transporter protein CTR1/ATP7A. Inductively coupled plasma mass spectrometry (ICP-MS) and principal component analysis (PCA) were used to identify the changes of heavy metal level in hippocampus and CSF after lead exposure. It was found that the change in copper level was most pronounced in the brain between 3 to 12 weeks post lead exposure. Ventriculo-cisternal (VC) perfusion in Sprague Dawley (SD) rat suggested that the ability of BCB to deliver copper from the CSF to blood was decreased after lead exposure. Confocal microscope showed evidence of the presence of excess copper in the choroid plexus cells leading to CTR1/ATP7A shifting toward the apical microvilli facing the CSF after lead exposure. Finally, transmission electron microscopy (TEM) was used for observation of the microstructure of choroid plexus showed altered mitochondrial morphology with decreased microvilli after lead exposure. Our data suggested that lead exposure may alter BCB cellular microscopic structure and its copper transport, clearance function that might further cause brain injury.

1. Introduction

lead is a heavy metal widely used in various industries, its release can permanently pollute the environment [1] .It has been well documented that lead exposure can develop multiple systemic adverse effects, including decreased intelligence quotient (IQ) [2, 3] cognitive impairment [4–6] memory decline [7, 8] and deficient attention[9–11] as well as known hematological toxicities.. In addition, recent studies have reported that lead exposure may aggravate neurodegenerative disorders, such as Alzheimer's and Parkinson's disease. However, the detailed mechanism has not been fully elucidated.

Previous studies have found that lead exposure can affect the distribution of some electrolytes ions and trace elements in the brain by causing changes in the expression of its transporters in brain barrier system. Data has shown that lead exposure can result in imbalance of brain’s iron homeostasis due to compromised blood-brain barrier (BBB) regulatory function [12]. It was found that more zinc ions were deposited in the intracellular zinc pool after lead exposure due to increased ZnT2 expression in choroidal epithelial cells by a yet unclear pathway [13]. Lead exposure can also alter the expression of copper transporters CTR1 and APT7A in Z310 cells, resulting in increased intracellular copper content [14]. However, these studies were focused on the change of ion or trace elements concentration after lead exposure resulting in disturbance of brain function through an unclear pathway. Because lead is a

divalent metal carries electronegativity and particle radius similarities with other ion or trace elements in the body [15, 16], and its absorption, distribution could mimic other divalent trace elements such as iron, zinc, calcium etc. There is no available data to demonstrate the significant changes of divalent metal ion or trace elements in the brain after lead exposure. Therefore, we hypothesized that lead may exert its neurotoxicity by affecting some key divalent ion distributions. This study designed to identify the changed divalent metals in the rats' hippocampus and CSF after lead exposure.

Our previous study found that lead exposure can cause copper accumulation in brain tissues of rats. The copper content in the striatum and hypothalamus of exposure group were 4.66 and 3.57 times of the control group [17]. Meanwhile, copper content in the hippocampal CA1 and DG regions were also higher and the copper transporter mRNA in the hippocampal CA1 region showed up-regulation after lead exposure [18]. It is known that copper is an essential trace element as co-factor for several enzymes, however, excessive copper can generate free radicals by interacting with oxygen [19]. The previous studies have demonstrated that copper disorder in brain has been linked to several neurodegenerative disorders, such as Parkinson's disease and Alzheimer's disease [20–22]. Copper homeostasis in the brain is regulated by brain barrier systems, one of which is BBB and the other is blood-CSF barrier (BCB) [23]. There are some reports suggested that free copper ions are mainly transported into brain via BBB, whereas BCB may play a critical role in regulating copper between peripheral blood and cerebrospinal fluid (CSF) [24–26]. The effects and potential mechanism of BCB on copper clearance after lead exposure are the chief research interest. The choroid plexus, an epithelial monolayer constituting to the BCB that produces the CSF, which is critical in regulating the essential trace elements between blood and CSF, eliminating metabolites or detrimental materials from extracellular fluid to the blood [27, 28]. Several molecules associated with copper transport proteins for uptake and efflux were also found to be expressed in choroidal epithelial cells [24, 25, 29]. The exact mechanism regarding lead exposure result in copper accumulation in the brain causing neurotoxicity is currently unclear. We hypothesized that lead exposure may induce BCB dysfunction by altering choroid plexus ultra-structure and expression of copper transporters which ultimately cause the dysfunction of copper clearance and its pathogenesis. Our study is to investigate the major changes of divalent metals in brain after lead exposure and explore its mechanisms.

2. Methods

2.1 Experimental animals' treatment and samples collection

SPF SD male rats, 21 days old weighting 60 ~ 70 g, were purchased from the Vital River Laboratory Animal Technology Co., Ltd (China, Beijing, Certificate number of animals: SCXK 2016-0006). Upon arrival, the rats were under immediately quarantine and were given a standard diet, purified drinking water and allowed to acclimatize for one week prior to the experimentation carried out in a room with standard laboratory conditions (12 hours light-dark cycle; 25 ± 2°C). The experiments were conducted in

accordance with the National Institutes of Health Guide for the Care and Use of Laboratory Animals, approved by the North China University of Science and Technology Animal Ethics Committee (No.201620). The total of 48 SD rats were randomized into control and lead group. The lead group were exposed to lead (50 mg/kg) for 3, 6, 9 and 12 weeks. Meanwhile, another 60 SD rats were divided into control, low-dose (50 mg/kg) and high-dose lead group (100 mg/kg) and exposed to lead for 12 weeks. The concentrations of lead selected were within the range of reported concentrations suffice in increasing tissue trace elements level and causing the study animals' neurotoxic effects, such as cognitive deficits, learning and memory disorders [30]. All the lead groups rats were given free water containing assigned dose of lead acetate. The control group rats were given free distilled water.

At the end of experiment, all the rats were sacrificed after anesthetized with ketamine/xylazine (75:10 mg/kg, l mg/Kg i.p.). CSF was collected, brain tissues were dissected on the ice plate and choroid plexus and hippocampus were harvested. The harvested hippocampus and choroid plexus from the 48 SD rats were stored at -80℃ freezer and later prepared for metal content detection. The choroid plexus of 18 SD rats were used for the mRNA expression analysis. The choroid plexus from nine of the SD rats were preserved in 4% paraformaldehyde and the other nine in 2.5% glutaraldehyde.

2.2 Detection of 12 elements concentrations by ICP-MS

The harvested tissues were digested with ultra-pure nitric acid in a microwave-accelerated reaction system. CSF was digested overnight with nitric acid in the over at 55℃. An Agilent 7500a was used to quantify elements concentrations. Digested samples were diluted 500 or 1000 times with 1.0% (vol/vol) HNO_3 to keep the reading within the range of the standard curve. The elements and their detection limit were shown in Table1.

Table 1
the detection limit of different elements ICP-MS

Elements	Detection limit(ng/L)
Cu	0.0300
V	0.0010
Cr	0.0040
Fe	0.0500
Ni	0.0800
Mg	0.0700
Co	0.0050
Ca	0.3000
Mo	0.0060
Zn	0.0400
Mn	0.0300
Pb	0.0001

Note. Determination limit: a single element standard was prepared into a series of concentrations until the minimum concentration met the linear equation R, not less than 0.998; the recovery rate of the lowest concentration ranged of 70–130%; the RSD of the solution at the lowest concentration point was continuously injected 6 times, not to exceed 10%. Detection limit: samples were allowed 3-fold dilation, then continuously tested 6 times.

Table 1
the different element of detection limit in ICP-MS

Element	Detection limit(ng/L)	Determination limit(μg/L)
Cu	0.020	6
V	0.700	-
Cr	0.080	2
Fe	0.300	100
Ni	0.100	6
Mg	0.040	1
Co	0.300	1
Ca	0.500	300
Mo	0.3	-
Zn	1.000	5
Mn	0.500	-
Pb	0.020	-

Note. Determination limit: a single element standard is prepared into a series of concentrations until the minimum concentration meets the linear equation R is not less than 0.998; the recovery rate of the lowest concentration point is in the range of 70–130%; the RSD of the solution at the lowest concentration point is continuously injected 6 times which should not more than 10%. Detection limit: The detection limit is diluted 3 times, and that needs to be continuously tested 6 times.

2.3 Immunofluorescence staining

Choroid plexus was fixed in 4% paraformaldehyde and permeabilized in 0.1% Triton X-100 at room temperature. After blocking with 1% bovine serum albumin (BSA) for 1 hour at room temperature, choroid plexus was incubated with anti-rabbit polyclonal CTR1, ATP7A primary antibodies (1:100) in 1% BSA at 4°C. Overnight, CTR1 and ATP7A were followed by incubation with dylight 488 labeled anti-mouse secondary antibodies (1:200). All of them were conducted at room temperature for 1 hour. To acquire images, slides were mounted on the stage of a Olympus FV1000 inverted confocal laser microscope and viewed through a × 100 oil-immersion objective (Plan Apo, × 100/1.40 oil, W.D. 0.13, cover glass thickness 0.17, DIC), with a 488-nm or 594-nm laser source for excitation. Each slide was examined under reduced transmitted-light illumination, and the area containing epithelium with underlying vasculature was chosen for analyses.

2.4 real-time PCR

The mRNA expression ctr1 and atp7a were quantified using real-time PCR. In brief, the total RNA was isolated from choroid plexus using TRIZOL reagent following manufacturer's introduction. An aliquot of

RNA (2 μg) was reverse-transcribed into cDNA by using a cDNA Reverse Transcription Kit (Roche, Swit). The expression of specific mRNA was assayed using fluorescence-based real-time PCR and reactions were performed using Fast SYBR PCR amplifier (Roche, Swit). Beta actin was chosen as a housekeeping gene. The amplification program was followed by 45 cycles of 95℃ for 5 seconds, 60℃ for 20 seconds and 72℃ for 15 seconds. Each real-time PCR reaction was run in triplicate. The cycle time (Ct) values of interested genes were normalized with that of the reference gene in the same sample to obtain delta Ct values.

The following primers were used:

ctr1: forward 5'-AGGTCTAGCTGACAGTCTCTCA-3'

reverse 5'-AAACTCGGCCTGCGTTTAGT-3'

atp7a:forward 5'-CCCTCAACAGCGTCGTCACT-3'

reverse 5'-ACTAGCAGCATCCCCAAAGG-3'

β-actin: forward 5'-GTGGATCAGCAAGCAGGAGT-3'

reverse 5'-CGCAGCTCAGTAACAGTCCG-3'

2.5 In situ VC perfusion

Relevant reagent concentrations for this experiment were selected in accordance with references. [25, 29, 31] Specific experimental methods were provided by Zheng Wei Laboratory of Purdue University. Briefly, rats were anesthetized and fixed in a stereotactic device. A midline skin incision was made from the forehead to the neck to expose the skull surface. A small drill bit (Plastics One Inc., Roanoke, VA) was used to make a hole in the skull for cannula placement. The cannula was implanted into the lateral ventricle according to the three data of following parameters: anterior 0.8 and posterior 0.8 cm, lateral line to midline 1.4 cm, and vertical 3.5 mm. This cannula was then used for micro pump- controlled lateral ventricular injection with artificial CSF. The artificial CSF was pre-mixed solution containing 35 μCi/ml of ^{64}Cu and 0.5 μCi/ml of ^{14}C-sucrose. The concentration of this mixture was 5 μM $CuCl_2$, which was delivered to the lateral ventricle at a rate of 28 μl/min that controlled by a micropump. (Harvard Syringe Pump, Model 11 Plus). Throughout the 90 minutes injection, 26G butterfly needles were inserted into the cistern magna at appropriate angles per 10 minutes intervals to collect CSF outflow. It was assumed that the density of artificial CSF is 1 g/ml and its weight was calculated from the volume of collected artificial CSF. In some cases, additional anesthesia to the rats were provided as needed in order to complete the procedures. The body temperature of the rats maintained at 37℃ using a heating pad during the experiments.

Calculation of various indicators:

Curve plot of perfusion time and radioactivity ratio of perfusion substance in collected liquid

Calculate the average of the radioactivity ratio of the perfusion material in the collected liquid when the plateau phase is reached. At least 5 of the arithmetic mean points were recorded for analysis.

Cout represent radioactivity of substances in the collected fluid

Cin represent radioactivity of substance during perfusion

Fin represent perfusion rate

RD represent that at the plateau phase of the radioactivity ratio between **Cin** and Cout of sucrose

2.6 Transmission electron microscopy

Two choroid plexus samples were utilized and fixed in 2.5% glutaraldehyde. The samples were combined with 1% osmium tetroxide, dehydrated through ascending series of acetone, and embedded in Epon812. Prior slicing them into ultra-thin sections, specimens were stained with lead citrate and uranyl acetate. The ultra-thin sections were viewed and photographed with a transmission electron microscope.

2.7 Morris water maze

To test learning and memory impairment, the Morris water maze (MWM) tasks were used to measure the rats' learning and memory ability. Visible (platform with a flag) and invisible (platform) trials were performed on lead group after lead exposure and the control group. For the visible trials, the hidden platform was placed below the water surface in the second quadrant and rats were gently placed in the pool at the fourth quadrant facing the pool wall. Rats were given 16 training (4 time per day/4 days) trials and escape latency is defined as the time required to find and climb onto the platform. During training, they had to rest on the platform for 30 seconds if the rat finds the platform before repeating the next training. If the rats were unable to locate a platform within 60 seconds, the time for this test is recorded as one minute. On the day 5, invisible platform trials were performed. Briefly, the hidden platform was removed, and the rats were placed in the water away from the prior platform location for a single trial lasting 60 s and recorded the frequencies of crossing the platform. Data was recorded using the Water Maze Video Tracking System (Zheng Hua Biological Instrument Equipment Co, Huai Bei, China). All cognitive tasks were performed between 10:00 and 17:00 hours during the day.

2.8 Statistical analysis

PCA was used to extract the principal component, to achieve the purpose of dimensionality reduction. The discriminant orthogonal least squares discriminant analysis (OPLSDA) was used to establish the distinguishing model between groups, and the differences in elemental spectra between the lead exposure group and the control group were captured. The model verifies the extracted principal component and finally determines the element distribution of the extracted principal component. Besides the PCA results, the data were shown as the mean ± SD; statistical analysis of the differences between

the lead and control groups were performed by using one-way ANOVA followed by a least significant difference test for multiple comparisons. A value of $p < 0.05$ was considered statistically significant.

3. Result

3.1 Lead induced obviously the learning and cognitive deficits.

By evaluating the spatial learning and memory performance using the Morris water maze test, it was found that the escape latency in lead exposure group was significantly longer at the third and the fourth day ($P < 0.001$, Fig. 1A). Further analysis found that the escape latency in the high-dose lead exposure group was longer compare with that of the low-dose lead group ($P < 0.01$, Fig. 1A). This data indicated that lead exposure was associated with decreased learning and memory ability in rats. In space exploration test, the average frequency of crossing the platform in lead exposure groups rats showed a decrease trend ($P < 0.001$, Fig. 1B) while the rats in high does lead group had the lowest frequency of crossing the platform. However, there was no statistical significance between the low and the high does lead groups. These results demonstrated that lead could gradually impair spatial orientation of rats. With higher concentration of lead exposure, there were signs of more severe injury to these rats' cognitive function.

3.2 Metal elements change in hippocampus of rats following lead exposure for 3, 6, 9, 12 weeks

We first used ICP-MS to detect the levels of metal elements in the hippocampus of rats. It was found that some divalent metal elements contents were so rare that they can be neglected. The nine divalent metal elements concentration changes in rat hippocampus were obtained for analysis. PCA was applied to extract the 9 elements and their changes in hippocampus after lead exposure. After 3 weeks of lead exposure, six main components were extracted from the hippocampus. Among them, factor 1(F1) included Ca, Cu, Ni, Mg, Fe and Zn accounting for 79.55% of the total variance. Three main components were extracted among lead and control group after 6 weeks lead exposure of which F1 included Ni, Fe and Cu accounting for 71.33% of the total variance. Three main components were extracted from the hippocampus of rats with 9 weeks lead exposure and F1 included Cu, Mg and Ca accounting for 79.39% of the total variance. Meanwhile, four principal components were extracted from all the elements of the rats' hippocampus after 12-week lead exposure and F1 included Ca, Fe, Zn, Mg and Cu accounting for 85.02% of the total variance. After 3–12 weeks of lead exposure, the principal metallic trace elements components analysis in rats' hippocampus indicated copper (Cu) detection. The copper concentration in the hippocampus showed significant changes as exhibited in Fig. 2.

3.3 Metal elements change in CSF of rats following lead exposure for 3, 6, 9, 12 weeks

By using the same metal measurement method as analyzing hippocampus, twelve kinds of divalent metals contents in CSF were identified. After 3 weeks of lead exposure, three main components of which in CSF were extracted. F1 included V, Cu and Fe accounting for 78.08% of the total variance. Five main components were extracted after 6 weeks lead exposure, F1 including Fe, Ni, V, Mo, Ca and Cu accounting for 85.36% of the total variance. After 9 weeks of lead exposure, five main components were extracted of which F1 including Cu, V, Ni, Cr, Mg and Ca accounting for 82.77% of the total variance. Five main components were extracted after 12 weeks of lead exposure that F1 including Ni, V, Cu, Fe and Mn accounting for 79.79% of the total variance. F1 extracted from the different exposure duration included V and Cu, and the differences are shown in Fig. 3.

These data suggested that there was significant change of copper level in the hippocampus and CSF of rats at each exposure duration, indicative that lead exposure might result in the copper disorder of rats' brain.

3.4 The accumulation of copper and lead in plasma and choroid plexus at different lead exposure duration

Our data indicated that lead exposure can affect copper level in CSF and hippocampus, which led us to try to elucidate its mechanism. Therefore, the copper and lead contents from plasma and choroid plexus were studied. The results were shown in Fig. 4. At every 3 weeks after lead exposure, both lead and copper levels in the plasma and choroid plexus were measured. These results showed that the lead and copper levels in the plasma increased after 3 to 12 weeks of lead exposure, conveying that there were increased lead and copper concentration in the peripheral blood after lead exposure.

As we know BCB is barrier regulating ion homeostasis between the brain and the blood, and the choroid plexus is an important component of the BCB. It can be found that at each point of lead exposure the levels of copper and lead were much higher than that in control. Copper and lead gradually accumulate in the choroid plexus during lead exposure for 3 to 12 weeks.

The lead and copper contents in plasma during lead exposure for 3 to 12 weeks were increased compared to the control group. These results predicted that the choroid plexus surface facing the peripheral blood would be at risk for contacting higher concentration of copper and lead. This changed environment may lead to the accumulation of lead and copper in the choroid plexus. Since there were increased lead and copper contents in the choroid plexus, they could affect the function of the choroid plexus. (for plasma n = 12 for choroid plexus n = 12 per group, one-way ANOVA for each group, $P < 0.05$ for overall acquisition, probe and reversal). In all panels, error bars represent mean ± SD. *$P < 0.01$ (lead group vs control group)

3.5 Lead exposure impacted the BCB ability of clearing copper.

The accumulation of lead in choroid plexus might disturb copper transporting from CSF to the blood in time, which might have caused the accumulation of copper in CSF. Therefor experiment was performed to investigate the lead exposure on copper clearance in choroid plexus. These studies used the ^{14}C and ^{64}Cu labeled artificial CSF for in situ VC perfusion to detect the ability of the BCB to transport copper. The space marker ^{14}C-sucrose, as macro molecule, was served to confirm the structural integrity of choroid plexus. ^{64}Cu and the space marker ^{14}C-sucrose artificial CSF were injected into the ventriculo cisternal. The CSF outflow was collected from the ventriculus quartum to test the radioactivity. When the ratio of radioactivity in the in/out CSF was increased which suggesting that there was much more ^{64}Cu or ^{14}C-sucrose accumulated in the CSF. The time course of ^{64}Cu and ^{14}C-sucrose was showed in Fig. 5 (A and B). The percentages of ^{64}Cu and ^{14}C-sucrose in the outflow of CSF reached a plateau at after 20 min of the initiation of perfusion. Data from Fig. 5C showed that ^{14}C-sucrose in the in/out CSF of the lead group showed no change between the lead exposure and control groups. The space marker ^{14}C-sucrose might be blocked up by the choroid plexus indicating that lead exposure has not caused a significant leakage in the choroid plexus. In contrast, a significantly higher percentage of ^{64}Cu was recovered from the CSF outflow in lead exposure animals as compared with controls (Fig. 5D), which implied a lower in vivo clearance of copper by the choroid plexus. The data in Fig. 5E revealed that the capacity of removing ^{64}Cu in the CSF through the choroid plexus was significantly lower in lead exposure rats than that of the controls ($p < 0.05$). Thus, it seemed likely that in vivo lead exposure significantly reduced the efflux of copper by the BCB. These data indicated that the increased level of copper in CSF after lead exposure might be due to lead interfering the function of the BCB.

3.6 Lead exposure resulted in the change of copper transporter expression in choroid plexus.

As shown in Fig. 6, CTR1 and ATP7A were distinctly expressed in the choroid plexus. In the control group, CTR1 was mainly expressed in the cytoplasm and cell membrane. The fluorescence intensity of CTR1 increased in the choroid plexus after lead exposure and primarily concentrated close to the apical border with a small portion along the basolateral membrane in the choroidal epithelial cells. In the control group, ATP7A was mainly expressed in the cytoplasm. The expression of ATP7A was significantly higher in the cytoplasm of choroid plexus with lead exposure than that in the control group. The intracellular ATP7A fluorescence intensity in high does lead group was higher than that in low does lead group. The plasma lead concentration increment correlated positively with the fluorescence intensity of CTR1 and ATP7A

Besides localization of copper transporter in choroid plexus by immunofluorescence confocal microscopy, we also tested the mRNA expressions of *ctr1* and *atp7a*. As was shown in Fig. 7, the mRNA expression of *ctr1* in the choroid plexus of low and high lead exposure group was upregulated by 2.69 ±

0.83 and 3.27 ± 0.82 folds respectively ($P < 0.05$). The atp7a mRNA expression were also significantly upregulated by 1.53 ± 0.33 and 1.91 ± 0.57 fold respectively ($P < 0.05$). However, there was no significantly changes of copper transporters expression between the low and high dose lead groups. Lead exposure may induce upregulation of ctr1, causing the excess copper absorption into the cell. Excess intracellular copper may cause stress response in the neurons in the brain. The excess intracellular copper might trigger the neuronal attempt to transport copper out of the cell, as evidenced by upregulation of atp7a expression.

3.7 Lead exposure resulted in choroid plexus morphology changes.

As were shown in Fig. 8, transmission electron microscopy was used to observe the cellular structure morphological alteration. Compared with the control group, the nucleus borders of the choroid plexus cells in the lead exposure group were blurred. The morphological structure of nuclear was abnormal with misaligned and diminished microvilli. The mitochondrial morphological structure was abnormal with fused ridges in some of the mitochondria and swollen in others. However, the ultra-structure changes were similar in the choroid plexus epithelial cells between the two lead exposure groups.

1. Nuclear
2. Microvilli
3. Mitochondria

Figure 8 The morphological changes of choroid plexus in lead group and control rats were observed by TEM. The cell nucleus image contained numerous visible cytoplasmic organelles such as mitochondrion (scale bars 2 μm) (Fig. 8 nucleus). The images with the blurred nucleus membrane observed in the figure belong to the lead groups. Surface of control epithelial cells are replete with microvilli. The microvilli in lead group cells were diminished and misaligned (scale bars 1 μm) (Fig. 8 Microvilli). Mitochondria in the control cells showed clear borders and internal ridges. However, the mitochondrial structure of the lead groups demonstrated partial ridge melting. (scale bars 1 μm) (Fig. 8 Mitochondria). (n = 4 per group)

4. Discussion

Copper serves as one of the critical trace elements that playing an essential role in brain cellular function and as a co-factor in certain enzyme reaction [38]. However, excessive copper may cause adverse systemic effects. It has been demonstrated that the level of copper in brain have a subtle relationship with the progress of some neurodegenerative diseases [39–41]. It is suggested that lead could indirectly alter copper metabolism that manifest as lead neurotoxicity. Since BCB serve as a regulatory site of maintaining the homeostasis of essential metal elements between the CSF and brain parenchyma [23, 42], a thorough understanding of BCB's function in regulating copper after lead exposure becomes imperative

Previous studies have clearly indicated that lead exposure might exert its neurotoxic effects indirectly by altering other metal elements status. [32–34]. However, detailed data related to the change of divalent metal elements in the brain after lead exposure are lacking. We used ICP-MS to identify the changes of several divalent metal elements in the rats' brain tissues after lead exposure from 3 to 12 weeks. Our data analysis revealed that there were significant changes in copper content in hippocampus and CSF after lead exposure. These results conveyed similar findings with the most prior *in vitro* and *in vivo* studies [35–37] which have clearly indicated that lead exposure can disturb the level of copper in rats' brain.

In the current study, our data showed that the levels of lead and copper in choroid plexus in lead exposed rats were higher than that in the control group. Meanwhile, in situ VC perfusion results provided additional evidence to confirm the clearance ability of choroids plexus. The similarity of ^{14}C-sucrose perfusion between lead and control groups rats indicated intact BCB structure without leakage after lead exposure. In contrast, the percentage of ^{64}Cu from the CSF outflow in lead exposure rats were much higher than that in the control group, indicative of lower copper clearance by BCB. Our data showed evidence of decreased copper transport from CSF to blood after lead exposure. Therefore, it became clearer that the BCB clearance function was critical in copper accumulation in the rats' brain after lead exposure. It has been shown that BCB can carry out a function to balance the copper homeostasis between peripheral blood and CSF by exchanging copper via transporters on the basolateral membrane of choroid plexus [23, 24, 43]. The transporters involved in cellular copper uptake and efflux processes are mainly copper transporter family (CTR) with high affinity for copper, P-type ATP copper transporters (ATPase, Cu^{2+} transporting, α polypeptide, β polypeptide, ATP7A / ATP7B) etc. Among them, CTR1 with three trans-membrane domain proteins can form a high density with low electron cloud at its active center, thereby taking up copper ions into the cell [43]. And ATP7A is responsible for transporting extra copper ions out of the cell [44, 45] to avoid the accumulation of excess copper ions in the cell. Our observations of CTR1 and ATP7A revealed that both tended to gather near the cell membrane and the fluorescence signal of the lead exposure group was higher than that of the control group. Also, in the subsequent real time PCR assay, the expression of ctr1 and atp7a in the choroid plexus after lead exposure was 3.27 and 1.91 times higher respectively than that of the control group. It has shown that there was an increased expression of atp7a in the rats' choroid plexus epithelium after lead exposure, which may be a stress related expression of mRNA in response to excess copper ions in the cells. The observation of more expression of ctr1 in choroid plexus epithelium after lead exposure than that of atp7a, might explain why there were excessive copper accumulation in these epithelial cells.

The choroid plexus is a complex capillary structure, a primary component of BCB. Its specialized epithelial enpendymal cell basal surface is in contact with peripheral blood. Its topical surface consists of cilia (microvilli) that secrets clear fluids as CSF [46]. It has been well established that the choroid plexus epithelial enpendymal cells are connected to each other through tight junctions or other biologic compounds. This tight connection between the choroid plexus epithelial cells makes its barrier function possible [47]. The unique properties of the choroid plexus epithelial enpendmal cell play important role in blockage of certain toxin or adverse substances into CSF. The integrity of the normal choroid plexus

physical structure is essential in maintaining its physiological function as BCB. Based on our current study, it is reasonable to postulate that lead might have damaged the ultra-structure of the choroid plexus lead to its biological dysfunction. This postulation is supported by the TEM observations of ultra-structure changes of rat choroid plexus epithelial cells after lead exposure, such changes demonstrated as diminished cilia (microvilli), distorted intracellular mitochondrial morphology. Combined with findings from previous studies, one might deduce that these choroid plexus cellular ultra-structures changes after lead exposure were caused by copper accumulation in these cells leading to their copper clearance ability that affected BCB function. The evidence of abnormal copper transporter protein expression in the choroid plexus epithelial cells also allow us to speculate that copper accumulation that the same pathogenesis occurred in the hippocampus, CSF and possibly in other brain tissues. The excessive copper in brain may be associated with the process of AD confirmed by the previous studies [48, 49] and the neurotoxicity caused by lead exposure was similar to that was seen in AD [50]. Our Morris Water Maze data confirmed that there were changes of memory, cognition and spatial orientation after rats exposed to lead. These findings suggested that copper accumulation after lead exposure could be one of the pathways for memory and cognitive disturbance. These data also agree with other lead neurotoxicity studies. [51, 52] However, no significant difference was found between the high does lead exposure group and the lower does group, indicative of lower dose lead exposure could sufficiently cause neurotoxicity in rats.

In summary, lead exposure can cause choroid plexus capillary epithelial cellular microscopic morphology changes, abnormal copper transporter expression leading to copper clearance dysfunction and copper accumulation in these epithelial cells and other brain tissues. The excess copper accumulation in the brain tissues could be involved in memory, cognition and spatial recognition decline in rats with lead exposure.

References

1. Flora G, Gupta D, Tiwari A. Toxicity of lead: A review with recent updates. Interdiscip Toxicol. 2012;5:47–58. https://doi.org/10.2478/v10102-012-0009-2.
2. Isaac CPJ, Sivakumar A, Kumar CRP. Lead levels in breast milk, blood plasma and intelligence quotient: A health hazard for women and infants. Bull Environ Contam Toxicol. 2012;88:145–9. https://doi.org/10.1007/s00128-011-0475-9.
3. Roy A, Hu H, Bellinger DC, Mukherjee B, Modali R, Nasaruddin K, Schwartz J, Wright RO, Ettinger AS, Palaniapan K, Balakrishnan K. Hemoglobin, lead exposure, and intelligence quotient: Effect modifcation by the DRD2 taq IA polymorphism, Environ. Health Perspect. 2011;119:144–9. https://doi.org/10.1289/ehp.0901878.
4. Mansouri MT, Muñoz-Fambuena I, Cauli O. Cognitive impairment associated with chronic lead exposure in adults, Neurol. Psychiatry Brain Res. 2018;30:5–8. https://doi.org/10.1016/j.npbr.2018.04.001.

5. Zhang L, Tu R, Wang Y, Hu Y, Li X, Cheng X, Yin Y, Li W, Huang H. Early-life exposure to lead induces cognitive impairment in elder mice targeting SIRT1 phosphorylation and oxidative alterations, Front Physiol 8 (2017). https://doi.org/10.3389/fphys.2017.00446.
6. Braun JM, Hoffman E, Schwartz J, Sanchez B, Schnaas L, Mercado-Garcia A, Solano-Gonzalez M, Bellinger DC, Lanphear BP, Hu H, Tellez-Rojo MM, Wright RO. M. Hernandez-Avila, Assessing windows of susceptibility to lead-induced cognitive deficits in Mexican children. Neurotoxicology. 2012;33:1040–7. https://doi.org/10.1016/j.neuro.2012.04.022.
7. 10.1046/j.1471-4159.1999.0722099.x
Murphy KJ, Regan CM, Low-level lead exposure in the early postnatal period results in persisting neuroplastic deficits associated with memory consolidation, Lippincott Williams & Wilkins, Inc, 1999. https://doi.org/10.1046/j.1471-4159.1999.0722099.x.
8. Boucher O, Burden MJ, Muckle G, Saint-Amour D, Ayotte P, Dewailly É, Nelson CA, Jacobson SW, Jacobson JL. Response inhibition and error monitoring during a visual Go/No-Go task in Inuit children exposed to lead, polychlorinated biphenyls, and methylmercury, Environ. Health Perspect. 2012;120:608–15. https://doi.org/10.1289/ehp.1103828.
9. Davis DW, Chang F, Burns B, Robinson J, Dossett D. Lead exposure and attention regulation in children living in poverty. Dev Med Child Neurol. 2004;46:825–31. https://doi.org/10.1017/S0012162204001446.
10. Hong SB, Im MH, Kim JW, Park EJ, Shin MS, Kim BN, Yoo HJ, Cho IH, Bhang SY, Hong YC, Cho SC. Environmental lead exposure and attention defcit/hyperactivity disorder symptom domains in a community sample of South Korean school-age children, Environ. Health Perspect. 2015;123:271–6. https://doi.org/10.1289/ehp.1307420.
11. Calderón J, Navarro ME, Jimenez-Capdeville ME, Santos-Diaz MA, Golden A, Rodriguez-Leyva I, Borja-Aburto V. F. Díaz-Barriga, Exposure to arsenic and lead and neuropsychological development in Mexican children. Environ Res. 2001;85:69–76. https://doi.org/10.1006/enrs.2000.4106.
12. An DZ, Ai JT, Fang HJ, Sun RB, Shi Y, Wang LL, Wang Q. Influence of iron supplementation on DMT1 (IRE)-induced transport of lead by brain barrier systems in vivo. Biomed Environ Sci. 2015;28:651–9. https://doi.org/10.3967/bes2015.091.
13. Fu X, Zeng A, Zheng W, Du Y. Upregulation of zinc transporter 2 in the blood-CSF barrier following lead exposure. Exp Biol Med. 2014;239:202–12. https://doi.org/10.1177/1535370213509213.
14. Zheng G, Zhang J, Xu Y, Shen X, Song H, Jing J, Luo W, Zheng W, Chen J. Involvement of CTR1 and ATP7A in lead (Pb)-induced copper (Cu) accumulation in choroidal epithelial cells. Toxicol Lett. 2014;225:110–8. https://doi.org/10.1016/j.toxlet.2013.11.034.
15. Rogers JT, Venkataramani V, Washburn C, Liu Y, Tummala V, Jiang H, Smith A, Cahill CM. A role for amyloid precursor protein translation to restore iron homeostasis and ameliorate lead (Pb) neurotoxicity, J Neurochem (2016) 479–94. https://doi.org/10.1111/jnc.13671.
16. Zhu G, Fan G, Feng C, Li Y, Chen Y, Zhou F, Du G, Jiao H, Liu Z, Xiao X, Lin F, Yan J. The effect of lead exposure on brain iron homeostasis and the expression of DMT1/FP1 in the brain in developing and

aged rats. Toxicol Lett. 2013;216:108–23. https://doi.org/10.1016/j.toxlet.2012.11.024.

17. Chen WW, Yan LC, Cao MY, Li XY, Pang SL, Wang Y, Zhang YS. Effect of lead exposure on the accumulation of copper and iron in central nervous system of rats. Chinese Journal of Industrial Hygiene Occupational Diseases. 2019;37(3):179–85. https://doi.org/10.3760/cma.j.issn.1001-9391.2019.03.004. (in Chinese).
18. Wang LY, Zhao XY, Meng Q, Qiu WX, Pu BX, Li S, Zhang YS. Expression of copper transport protein in different regions of hippocampus of lead-exposed rats. Journal Toxicol. 2019;33:361–5. https://doi.org/10.3760/cma.j.issn.1001-9391.2019.03.004. (in Chinese). (05).
19. Berterame NM, Martani F, Porro D, Branduardi P. Copper homeostasis as a target to improve Saccharomyces cerevisiae tolerance to oxidative stress. Metab Eng. 2018;46:43–50. https://doi.org/10.1016/j.ymben.2018.02.010.
20. Nishimuta M, Masui K, Yamamoto T, Ikarashi Y, Tokushige K, Hashimoto E, Nagashima Y, Shibata N. Copper deposition in oligodendroglial cells in an autopsied case of hepatolenticular degeneration. Neuropathology. 2018;38:321–8. https://doi.org/10.1111/neup.12456.
21. Barnham KJ, Bush AI. Metals in Alzheimer's and Parkinson's Diseases. Curr Opin Chem Biol. 2008;12:222–8. https://doi.org/10.1016/j.cbpa.2008.02.019.
22. Hsu HW, Bondy SC, Kitazawa M. Environmental and dietary exposure to copper and its cellular mechanisms linking to Alzheimer's disease. Toxicol Sci. 2018;163:338–45. https://doi.org/10.1093/toxsci/kfy025.
23. Zheng W, Monnot AD. Regulation of brain iron and copper homeostasis by brain barrier systems: implication in neurodegenerative diseases. Pharmacol Ther. 2012;133(2):177–88. https://doi.org/10.1016/j.pharmthera.2011.10.006.
24. Choi BS, Zheng W. Copper transport to the brain by the blood-brain barrier and blood-CSF barrier. Brain Res. 2009;1248:14–21. https://doi.org/10.1016/j.brainres.2008.10.056.
25. Monnot AD, Behl M, Ho S, Zheng W. Regulation of brain copper homeostasis by the brain barrier systems: effects of Fe-overload and Fe-deficiency. Toxicol Appl Pharmacol. 2011;256(3):249–57. https://doi.org/doi:10.1016/j.taap.2011.02.003.
26. W. Zheng, Toxicology of choroid plexus: Special reference to metal-induced neurotoxicities, Microsc. Res. Tech. 52 (2001) 89–103. https://doi.org/10.1002/1097-0029(20010101)52:1<89::AID-JEMT11>3.0.CO;2-2.
27. Zheng W, Aschner M, Ghersi-Egea JF. Brain barrier systems: a new frontier in metal neurotoxicological research. Toxicol Appl Pharmacol. 2009;53:820–33. https://doi.org/10.1016/s0041-008x(03)00251-5.
28. Chen DB, Feng L, Lin XP, Zhang W, Li FR, Liang XL, Li XH. Penicillamine increases free copper and enhances oxidative stress in the brain of toxic milk mice, PLoS One 7 (2012). https://doi.org/10.1371/journal.pone.0037709.
29. Deane R, Zheng W, Zlokovic BV. Brain capillary endothelium and choroid plexus epithelium regulate transport of transferrin-bound and free iron into the rat brain. J Neurochem. 2004;88:813–20.

https://doi.org/10.1046/j.1471-4159.2003.02221.x.

30. Molina RM, Phattanarudee S, Kim J, Thompson K, Wessling-Resnick M, Maher TJ, Brain JD. Ingestion of Mn and Pb by rats during and after pregnancy alters iron metabolism and behavior in offspring. Neurotoxicology. 2011;32(4):413–22. [DOI: 10.1016/j.neuro.2011.03.010].
31. Wang XQ, Li GJ, Zheng W. Efflux of iron from the cerebrospinal fluid to the blood at the blood-CSF barrier: Effect of manganese exposure. Exp Biol Med. 2008b;233:1561–71. https://doi.org/10.3181/0803-RM-104.
32. Rahman A, Khan KM, Rao MS. Exposure to low level of lead during preweaning period increases metallothionein-3 expression and dysregulates divalent cation levels in the brain of young rats. Neurotoxicology. 2018;65:135–43. https://doi.org/10.1016/j.neuro.2018.02.008.
33. Wani AL, Ahmad A, Shadab GGHA, Usmani JA. Possible role of zinc in diminishing lead-related occupational stress — a zinc nutrition concern, (2017). https://doi.org/10.1007/s11356-017-8569-5.
34. Qian Y, Mikeska G, Harris ED, Bratton GR, Tiffany-Castiglioni E. Effect of lead exposure and accumulation on copper homeostasis in cultured C6 rat glioma cells, Toxicol. Appl Pharmacol. 1999;158:41–9. https://doi.org/10.1006/taap.1999.8657.
35. Qian Y, Tiffany-Castiglioni E, Harris ED. Copper transport and kinetics in cultured C6 rat glioma cells, Am J Physiol - Cell Physiol 269 (1995). https://doi.org/10.1152/ajpcell.1995.269.4.c892.
36. Sierra EM, Rowles TK, Martin J, Bratton GR, Womac C, Tiffany-Castiglioni E. Low level lead neurotoxicity in a pregnant guinea pigs model: neuroglial enzyme activities and brain trace metal concentrations. Toxicology. 1989;59:81–96. https://doi.org/10.1016/0300-483X(89)90158-3.
37. Qian Y, Zheng Y, Ramos KS, Tiffany-Castiglioni E. The involvement of copper transporter in lead-induced oxidative stress in astroglia. Neurochem Res. 2005;30:429–38. https://doi.org/10.1007/s11064-005-2677-1.
38. Horn D, Barrientos A. Mitochondrial copper metabolism and delivery to cytochrome c oxidase. IUBMB life. 2008;60(7):421–9. https://doi.org/10.1002/iub.50.
39. Waggoner DJ, Bartnikas TB, Gitlin JD. The role of copper in neurodegenerative disease. Neurobiol Dis. 1999;6:221–30. https://doi.org/10.1006/nbdi.1999.0250.
40. Squitti R, Ghidoni R, Simonelli I, Ivanova ID, Colabufo NA, Zuin M, Benussi L, Binetti G, Cassetta E, Rongioletti M, Siotto M. Copper dyshomeostasis in Wilson disease and Alzheimer's disease as shown by serum and urine copper indicators. J Trace Elem Med Biol. 2018;45:181–8. https://doi.org/10.1016/j.jtemb.2017.11.005.
41. Giampietro R, Spinelli F, Contino M, Colabufo NA. The Pivotal Role of Copper in Neurodegeneration: A New Strategy for the Therapy of Neurodegenerative Disorders. Mol Pharm. 2018;15:808–20. https://doi.org/10.1021/acs.molpharmaceut.7b00841.
42. Kuo YM, Gybina AA, Pyatskowit JW, Gitschier J, Prohaska JR. Copper transport protein (Ctr1) levels in mice are tissue specific and dependent on copper status. J Nutr. 2006;136(1):21–6. https://doi.org/10.1093/jn/136.1.21.

43. Harris ED. Copper Homeostasis: The Role of Cellular Transporters. Nutr Rev. 2009;59:281–5. https://doi.org/10.1111/j.1753-4887.2001.tb07017.x.
44. Kühlbrandt W. Biology, structure and mechanism of P-type ATPases. Nat Rev Mol Cell Biol. 2004;5:282–95. https://doi.org/10.1038/nrm1354.
45. Qian Y, Tiffany-Castiglioni E, Harris ED. A Menkes P-type ATPase involved in copper homeostasis in the central nervous system of the rat, Mol. Brain Res. 1997;48:60–6. https://doi.org/10.1016/S0169-328X(97)00083-1.
46. Monnot AD, Zheng G, Zheng W. Mechanism of copper transport at the blood-cerebrospinal fluid barrier: Influence of iron deficiency in an in vitro model. Exp Biol Med. 2012;237:327–33. https://doi.org/10.1258/ebm.2011.011170.
47. Damkier HH, Brown PD, Praetorius J. Cerebrospinal fluid secretion by the choroid plexus. Physiol Rev. 2013;93:1847–92. https://doi.org/10.1152/physrev.00004.2013.
48. 10.1016/j.neurobiolaging.2014.12.005
Hou P, Liu G, Zhao Y, Shi Z, Zheng Q, Bu G, Xu H, Y wu Zhang, The role of copper and the copper-related protein CUTA in mediating APP processing and Aβ generation, Neurobiol. Aging. 36 (2015) 1310–1315. https://doi.org/10.1016/j.neurobiolaging.2014.12.005.
49. Brewer GJ. Copper toxicity in Alzheimer's disease: Cognitive loss from ingestion of inorganic copper. J Trace Elem Med Biol. 2012;26:89–92. https://doi.org/10.1016/j.jtemb.2012.04.019.
50. Zhou CC, Gao ZY, Wang J, Wu MQ, Hu S, Chen F, Liu JX, Pan H, Yan CH. Lead exposure induces Alzheimers's disease (AD)-like pathology and disturbes cholesterol metabolism in the young rat brain. Toxicol Lett. 2018;296:173–83. https://doi.org/10.1016/j.toxlet.2018.06.1065.
51. Wang T, Guan RL, Liu MC, Shen XF, Chen JY, Zhao MG, Luo WJ. Lead Exposure Impairs Hippocampus Related Learning and Memory by Altering Synaptic Plasticity and Morphology During Juvenile Period. Mol Neurobiol. 2016;53:3740–52. https://doi.org/10.1007/s12035-015-9312-1.
52. Moosavirad SA, Rabbani M, Sharifzadeh M, Hosseini-Sharifabad A. Protective effect of Vitamin C, vitamin B12 and omega-3 on leadinduced memory impairment in rat. Res Pharm Sci. 2016;11:390–6. https://doi.org/10.4103/1735-5362.192490.

Figures

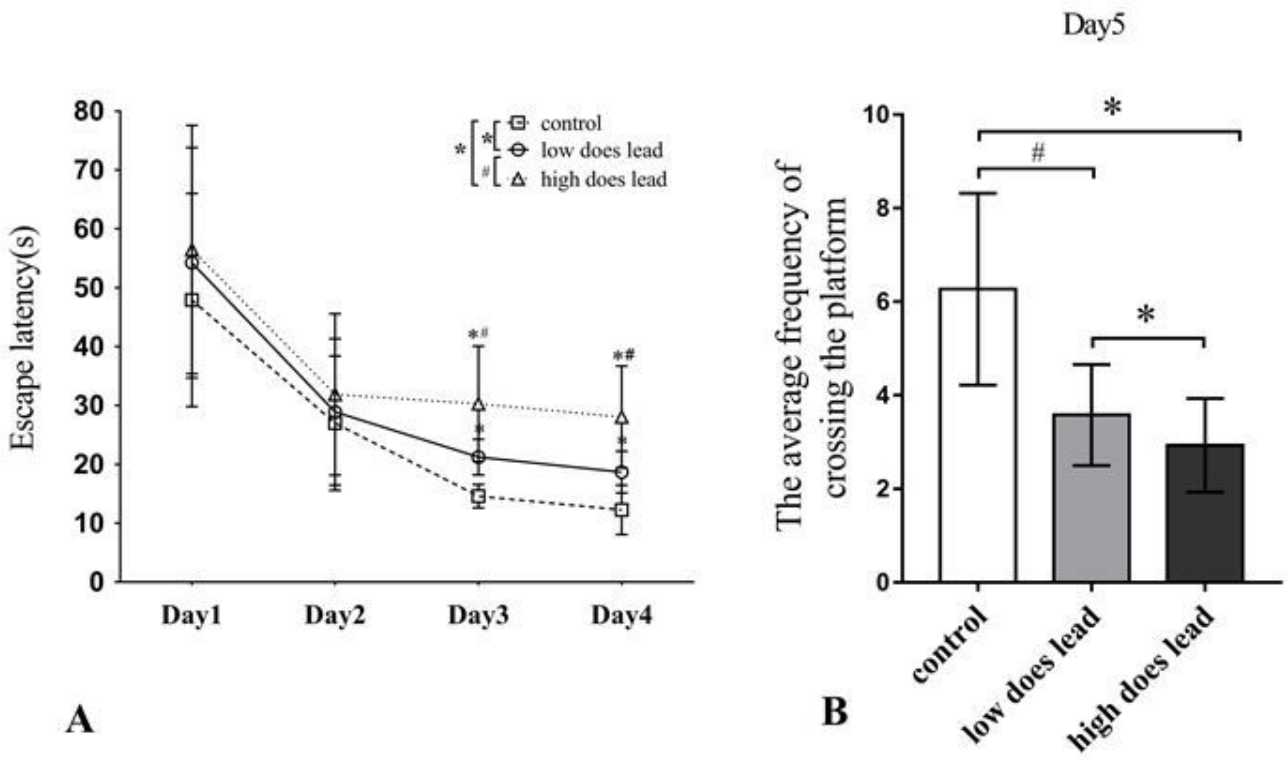

Figure 1

Lead induced learning and cognitive deficits. (A) Lead exposure group rats showed decreased spatial learning/memory acquisition, (B) Day 5 data of the memory of locating the platform. The rats in lead exposure group performed worse relative to the control group (n=12 rats per group), one-way ANOVA for each group, P<0.05 for overall acquisition, probe and reversal). In all panels, error bars represent mean±SD. *P<0.001 (low does lead exposure group vs control). #P<0.01 (high does lead exposure group vs low dose lead exposure group).

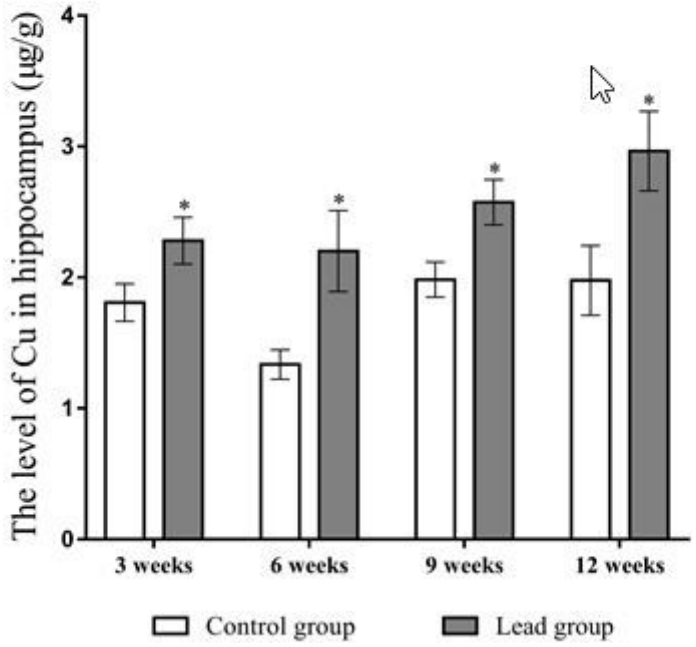

Figure 2

The effect of lead exposure on the copper level in hippocampus. The copper contents of hippocampus during lead exposure for 3 to 12 weeks was increased significantly compared to the control group. (n=12 per group, one-way ANOVA analysis for two groups, P<0.05 for overall acquisition, probe and reversal). In all panels, the error bars represent mean ± SD. *P<0.01 (lead group vs control group)

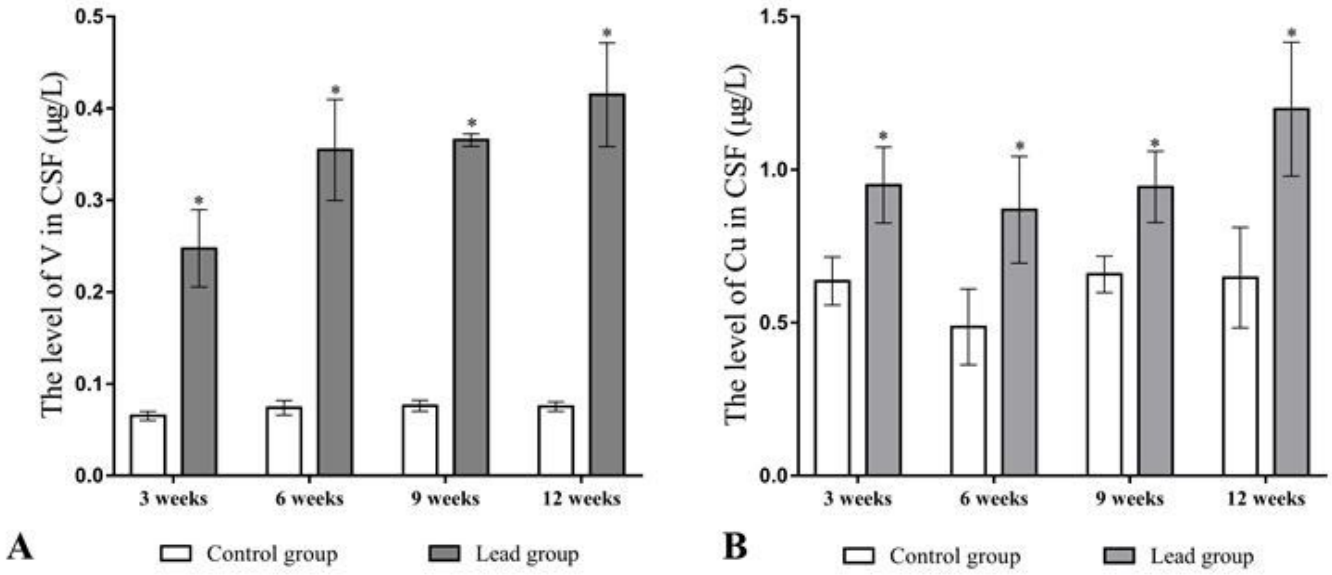

Figure 3

The effect of lead exposure on the level of copper and vanadium in CSF. Both the copper and vanadium contents of hippocampus during lead exposure for 3 to 12 weeks was increased compared to the control group. (n=12 per group, one-way ANOVA analysis for two groups, P<0.05 for overall acquisition, probe and reversal). In all panels, the error bars represent mean ± SD. *P<0.01 (lead group vs control group)

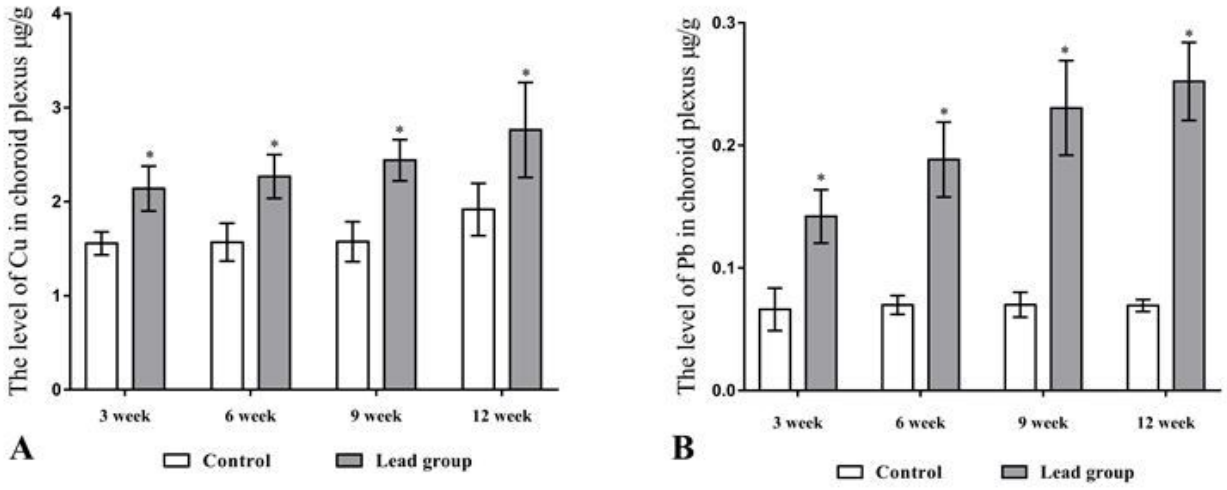

Figure 4

The effect of lead exposure on the level of copper and lead in choroid plexus (A-B). The lead contents of choroid plexus after 3-12 weeks of lead exposure were increased compared to the control group. The copper contents of choroid plexus during the lead exposure for 3 to 12 weeks were significantly increased compared with the control group, more so over the exposure duration.

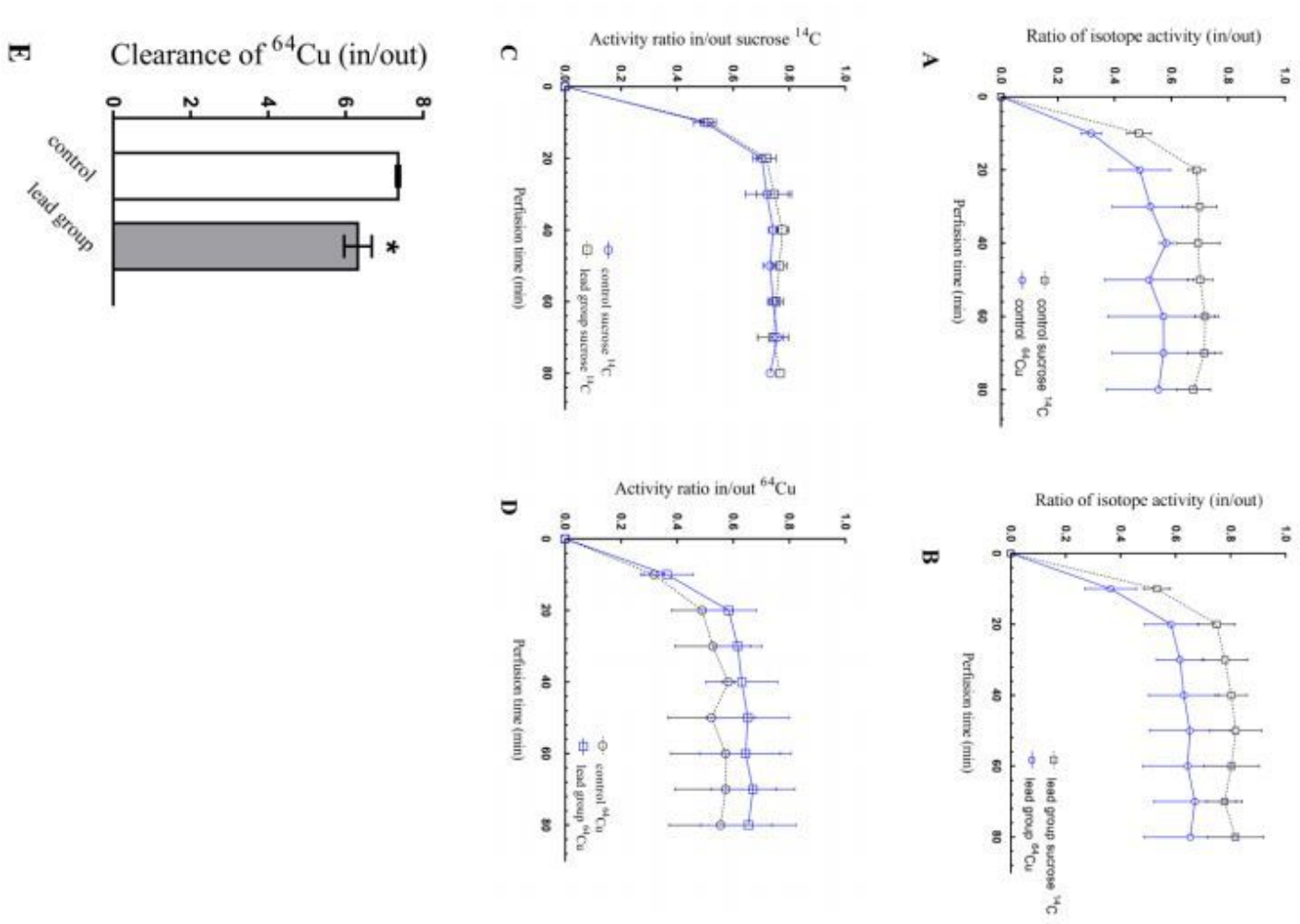

Figure 5

Representations of the copper clearing ability in lead exposure group and control group. The radioactivity from perfusion fluid and collected CSF were measured by gamma-liquid scintillation counter (A-B). The radioactivity of 14C and 64Cu (in/out) measurement were different for control group and the lead exposure group. The radioactivity reached plateau when the injection duration was at 20 minutes (C-D). There was no significant difference in the radioactivity between the isotopes used in the control group and lead exposure group. In the collected CSF, the radioactivity of the lead exposure group was higher than that was in the control. (E) The BCB ability for clearing 64Cu were decreased compared with control group, one-way ANOVA for each group. In all panels, error bars represent mean±SD. n=5, *P<0.01 (lead group vs control group).

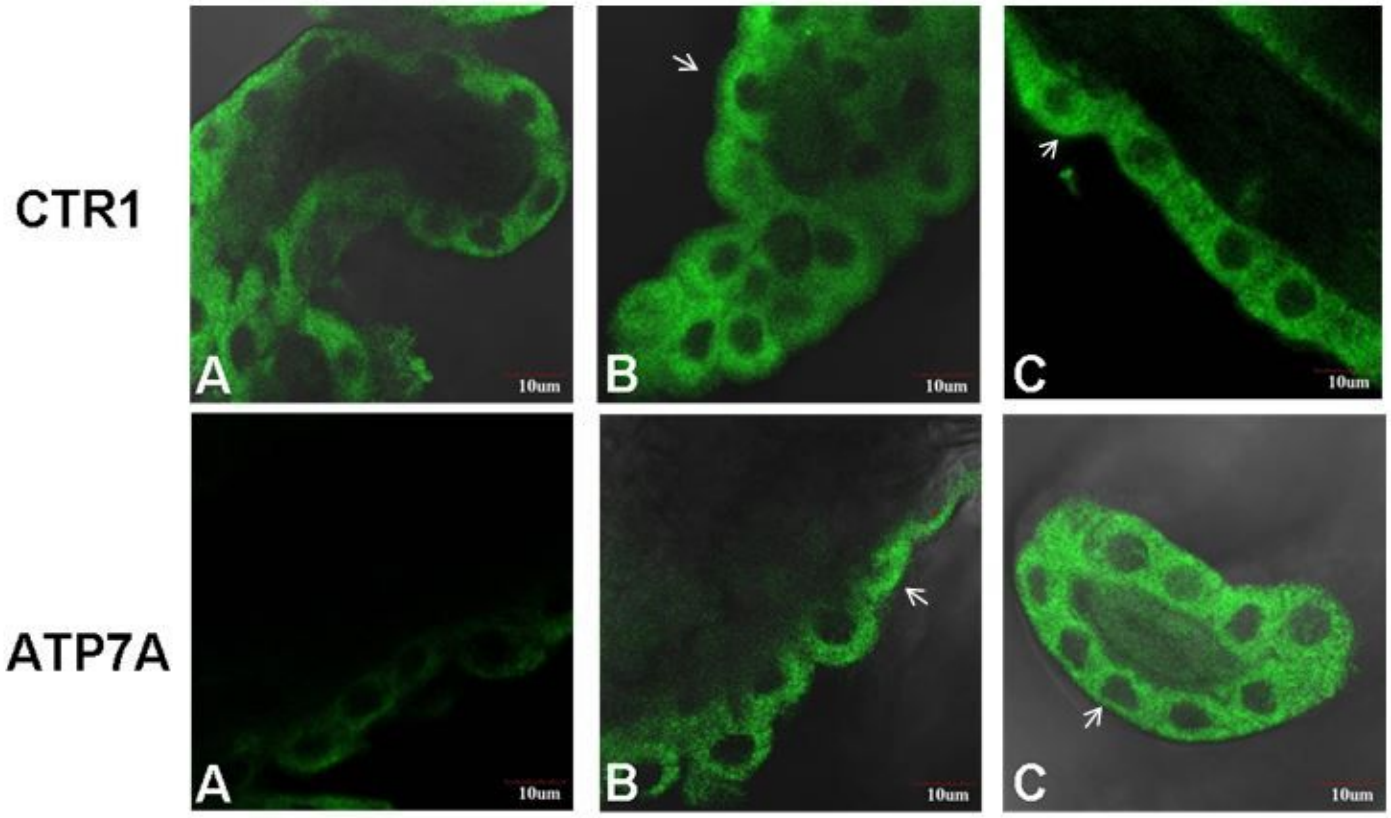

Figure 6

Expression of CTR1 and ATP7A in choroid plexus tissues after lead exposure. Choroid plexus tissues were dissected from the lateral ventricles. Copper transporter expression in choroid plexus after lead exposure were observed under the confocal microscope. (A-C) Representative images of immunostaining of copper transporter CTR1 and ATP7A (epithelial microvilli in green fluorescence) in choroid plexus from the control group, low does lead group and high does lead group (scale bars indicated 10μm). (n=3 per group).

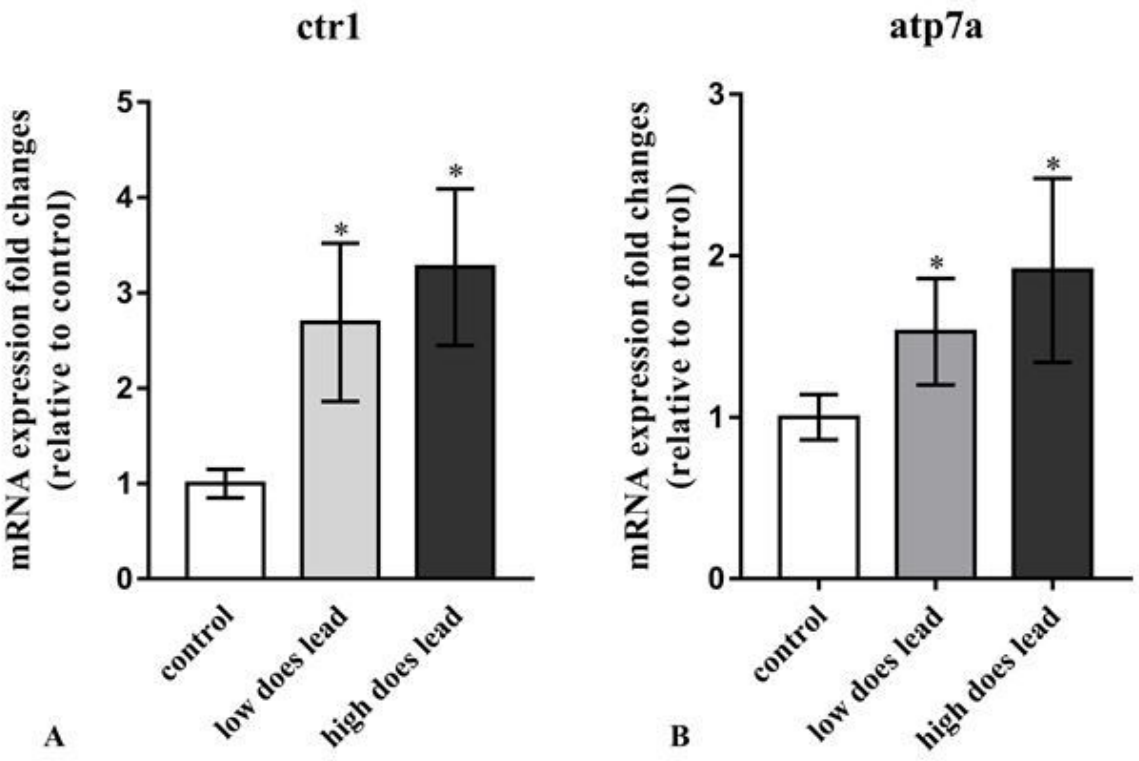

Figure 7

The mRNA expression of copper chaperone in choroids plexus after lead exposure. (A-B) mRNA of ctr1 and atp7a dependent genes in choroid plexus of lead groups (fold change relative to controls. n=8 per group. one-way ANOVA for each group. In all panels, error bars represent mean±SD. *P<0.05 (lead group vs control).

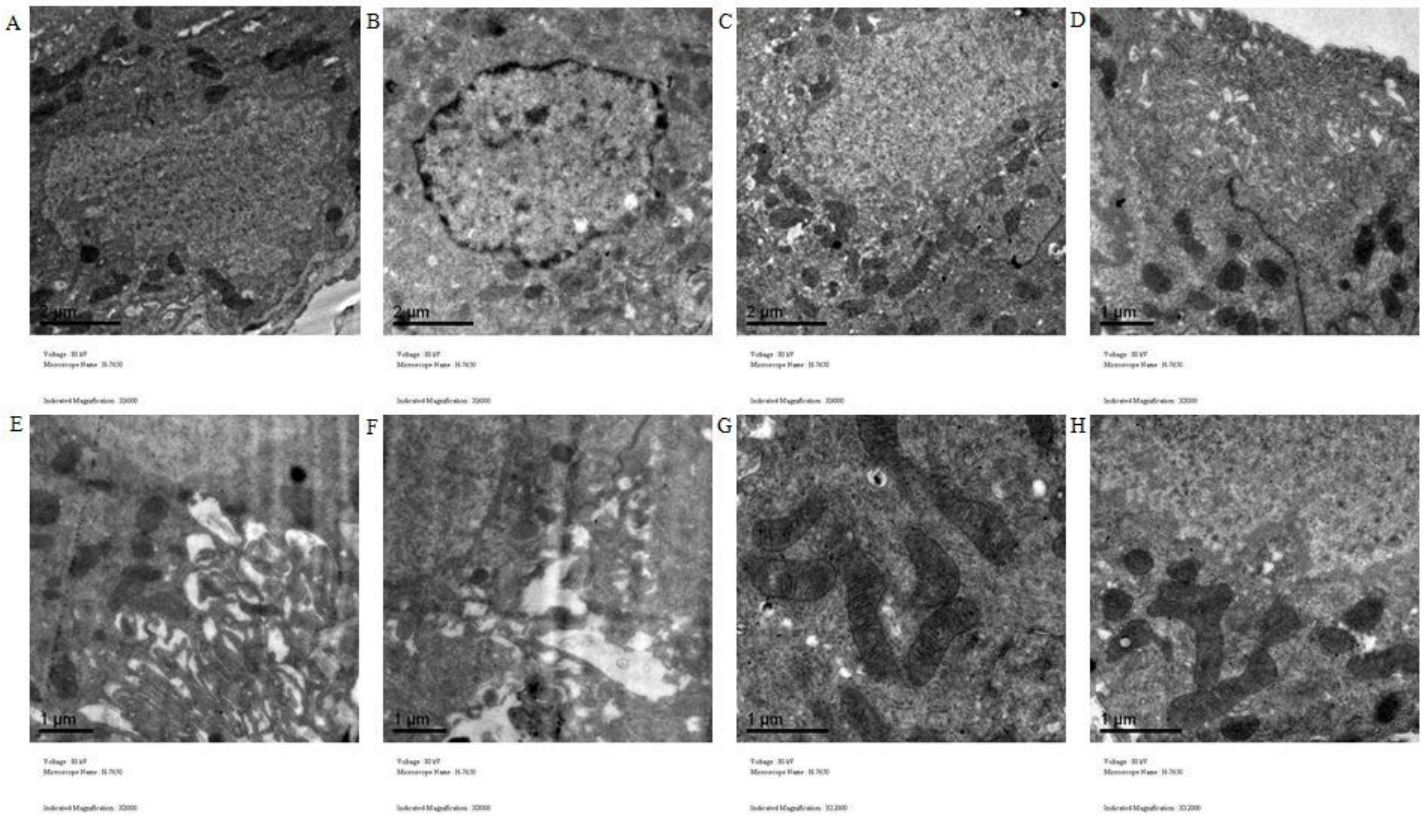

Figure 8

The morphological changes of choroid plexus in lead group and control rats were observed by TEM. The cell nucleus image contained numerous visible cytoplasmic organelles such as mitochondrion (scale bars 2μm) (Fig.8 nucleus). The images with the blurred nucleus membrane observed in the figure belong to the lead groups. Surface of control epithelial cells are replete with microvilli. The microvilli in lead group cells were diminished and misaligned (scale bars 1μm) (Fig.8 Microvilli). Mitochondria in the control cells showed clear borders and internal ridges. However, the mitochondrial structure of the lead groups demonstrated partial ridge melting. (scale bars 1μm) (Fig.8 Mitochondria). (n=4 per group)

Supplementary Files

This is a list of supplementary files associated with this preprint. Click to download.

- highlights.docx
- Graphicalabstract.pptx